RAPID PROTOTYPING OF 3D PRINTED MEMS ARRAYS ON FLEXIBLE SUBSTRATES

Regan Kubicek, Sukjun Kim, and Sarah Bergbreiter*
Department of Mechanical Engineering, Carnegie Mellon University, Pittsburgh, PA, USA

ABSTRACT
This paper presents the first 3D printed MEMS sensor arrays on flexible substrates. A novel fabrication method integrates direct 3D printing on flexible substrates with metal deposition and laser ablation to rapidly prototype arrays of 3D MEMS devices in a couple of hours instead of days using conventional methods. A secondary contribution introduces a novel bio-inspired MEMS strain sensor that closes a switch at a designed strain threshold, providing a low-latency digital indicator for when a particular strain has been reached.

KEYWORDS
Sensor Arrays, 3D Printing, MEMS, Flexible Electronics, Bio-inspired, Two-Photon Polymerization (TPP)

INTRODUCTION
Fabricating MEMS devices on flexible substrates enables compliant, lightweight device integration essential to applications from flexible displays [1] to health monitoring [2]. Sensing 'skins' composed of MEMS sensor arrays on flexible substrates are particularly appealing for numerous robotic applications from humanoids [3] to UAVs [4]. However, creating flexible sensor arrays similar to those found in biological systems like our own skin involves numerous engineering challenges. While larger (> 1 cm) flexible sensor arrays have become more common [5], microscale MEMS sensors are typically limited to rigid silicon wafers to take advantage of standard microfabrication processes. In addition, traditional MEMS sensor arrays typically require significant design and fabrication time from days to months.

Some of these challenges have previously been tackled using transfer printing – an approach designed to transfer MEMS devices fabricated on a rigid donor substrate to a flexible receiver substrate through bonding [6]. While this solves the problem of putting MEMS on a flexible substrate, transfer printing still has fabrication limitations, misalignment challenges, and requires significant cleanroom time to fabricate the MEMS devices [7]. Rapid prototyping through 3D printing could provide benefits, including increased design complexity and a reduction in fabrication time. Polymer 3D structures with microscale features have previously been printed on flexible polyethylene terephthalate (PET) sheets using two-photon polymerization (TPP) [8, 9]. In addition, electrical functionality has been added to TPP-printed structures using metal sputtering to fabricate 3D MEMS actuators, but these were limited to rigid substrates [10].

This work builds on these previous techniques to rapidly fabricate MEMS sensor arrays on a highly flexible substrate. We take advantage of rapid prototyping by using the two-photon polymerization process and extend its utility through the design of new processes to print complex structures (including long overhangs without supports) directly onto 50 μm thin PET sheets. Sputtered metal is used to provide electrical conductivity to the sensors similar to the approach used in [10], but in this work, laser ablation of deposited metal is demonstrated as an alternative approach to chemical etching or shadow masking to achieve electrical isolation. This rapid prototyping process enables MEMS devices to be directly printed on flexible substrates, drastically decreasing fabrication time, and reducing cost, while also presenting 3D devices that are not achievable or challenging to achieve with traditional 2D processes.

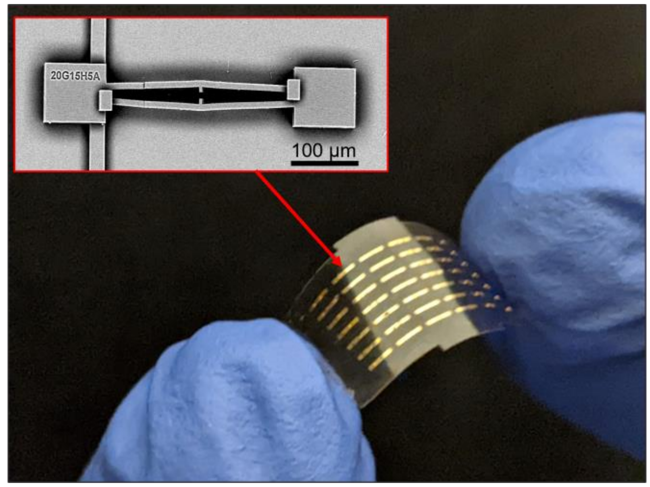

Figure 1. Flexible 42 sensor array directly 3D printed on 50µm thick PET. One example of the bio-inspired MEMS strain switch sensor is shown in the inset.

To demonstrate this novel fabrication process, we also present a new strain sensor inspired by mechanosensors found on the wings of the hawkmoth *Manduca Sexta* called campaniform sensilla [11, 12]. Campaniform sensilla are different from most engineered sensors in that they do not provide a continuous analog signal but instead send neural spikes in response to particular strain stimuli [13]. In previous work, we presented a macro scale strain sensor that outputs a discrete analog signal [14]. This work extends this idea and dramatically reduces the size of the sensor to enable both higher density arrays as well as greater substrate compliance (Figure 1). The result is a strain sensor that activates at a particular strain threshold, acting as a switch. When combined with a simple voltage divider, the contact switch provides a large enough change in voltage to be captured by a digital input on a microcontroller.

FABRICATION
This fabrication process in this work combines two-photon polymerization, metal sputtering, and laser ablation to facilitate rapid prototyping of 3D MEMS on flexible substrates. Structures are

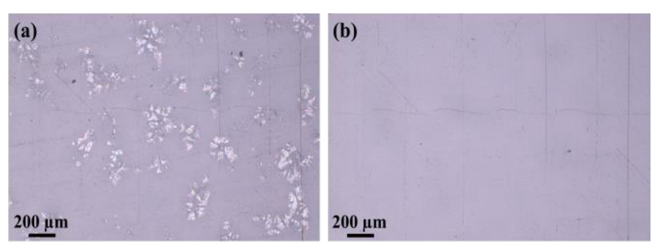

Figure 2. PET adhered to glass slide with Crystalbond 555 (a) Rapid cooling creates artifacts in the Crystalbond which can cause interface finding issues. (b) Slow cooling of Crystalbond provides an optically clear sample that is ideal for automatically finding the interface.

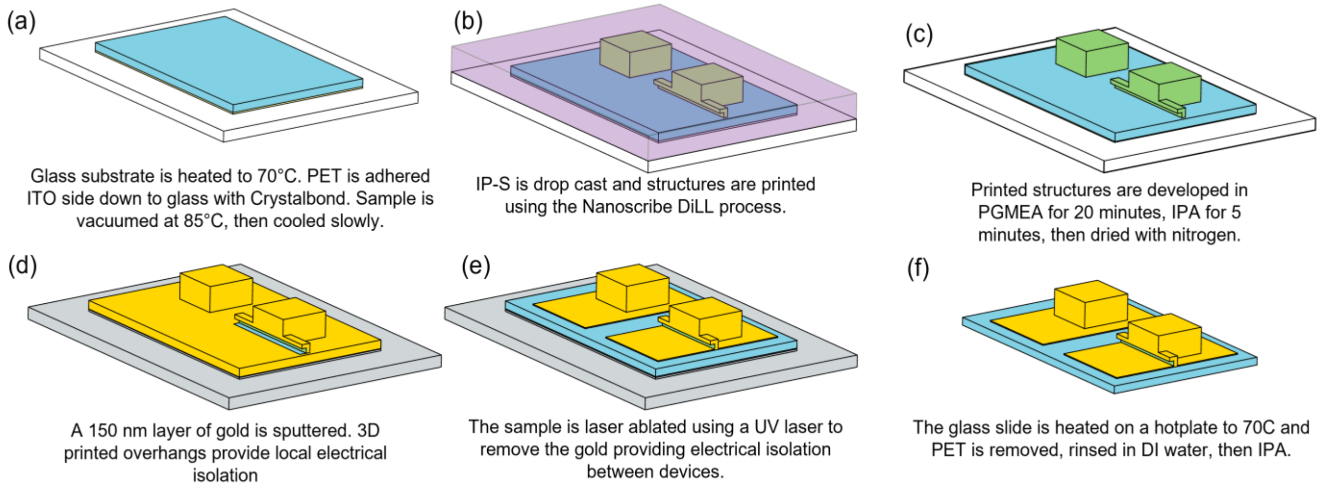

Figure 3: A rapid fabrication process produces flexible MEMS from concept to device in hours. Note the electrical isolation in (e) using 3D overhanging structures and laser etching. Overhangs provide local electrical isolation and laser etching provides global electrical isolation.

directly printed on PET using TPP with a Nanoscribe Photonic Professional GT+ (Nanoscribe Gmbh). In the first step of the fabrication process, an ITO-coated PET sheet is cut to shape using an LPKF U4 laser. During this process, fiducials are added for alignment during printing and for final laser ablation. The substrate used in the fabrication process is an off-the-shelf 300 Ω/sq, 50µm thick Indium Tin Oxide (ITO) coated PET (Sheldahl). The ITO is not used for its conductivity but instead provides a refractive index contrast to the adhesive layer which is required for interface finding in TPP.

One challenge in handling flexible substrates using existing tools is keeping the substrate flat during processing. To accomplish this, Crystalbond 555 is used as an adhesion layer to bond the substrate flat during the fabrication process. A 25mm x 25mm x 0.7 mm silica glass slide is cleaned with IPA and placed on a hotplate at 70°C. Crystalbond 555 is applied to the glass slide, and the PET is placed ITO side down, allowing the capillary forces to pull it uniformly on the glass. The prepared slide is then placed in a vacuum oven at 85°C with a gauge pressure of 25 inHg for 30 minutes to remove air bubbles trapped under the PET. Trapped bubbles can cause interface finding issues during printing and deformations in the substrate while under a high vacuum during subsequent sputtering.

The sample is placed back on a hotplate at 60°C and covered with a petri dish. The hotplate is turned off and left to cool for 20 minutes to room temperature. This slow cooling is a crucial step that prevents artifacts from forming in the Crystalbond, leaving an optically clear layer under the PET that is ideal for interface finding during the 3D printing process (Figure 2). Automatically finding an interface is a critical step in printing using TPP. A weak interface signal can result in structures printed too deep or above the substrate. When printing larger structures with multiple split blocks, an insufficient interface or artifact can lead to misalignment between blocks. By removing bubbles and slowly cooling the Crystalbond 555, we are left with an ITO/Crystalbond interface that provides a robust and consistent interface signal across the entire substrate allowing for larger arrays to be printed. It should also be noted that the ITO/Crystalbond interface is on the bottom of the substrate, and structures are printed on the top. As a result, the z-offset must be adjusted to account for the PET thickness [9]. This offset is found by printing test structures and increasing the z-offset until the structures are visible on the top of the PET. A z-offset of 52 µm was added in this work to print structures on the non-ITO side.

Once the substrate was prepared, the Nanoscribe Dip-in Laser Lithography (DiLL) [15] process was used to print 3D structures. IP-S resist was drop cast onto the PET (Figure 3b), and the structures were printed with the 25X objective and a laser power of 50 mW. The laser power used for the base layer was dropped to 35 mW to alleviate bubbling at the IP-S/PET interface. Another challenge addressed in this fabrication process was printing long (e.g., > 1 mm) overhanging structures. Printing with IP-S resist traditionally requires support structures to prevent drift and misalignment during printing. To print large structures in general, the Nanoscribe needs to break printing steps into blocks – the 25x objective used in this work can print up to a 280 x 280 µm square area at one time before

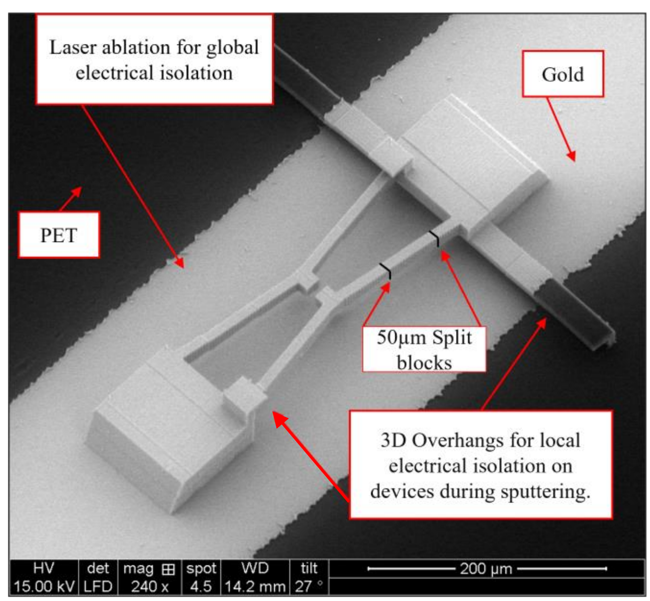

Figure 4: SEM of strain switch shows local and global electrical isolation as well as the long unsupported structures. Long overhanging structures are achieved by reducing split block size to 50µm.

the stage moves to print the next square. These areas are called 'split blocks'. We found that long overhanging structures could be achieved by reducing the split block size to 50 µm, which prevents drift in IP-S during printing (Figure 4). After printing, the structures were developed in PGMEA for 20 min and rinsed in IPA.

To provide electrical conductivity to the 3D polymer structures, gold was then sputtered to a thickness of 150 nm using a Perkin Elmer 6J Sputtering System. Two approaches were used to pattern the gold and provide electrical isolation. Previous work in used overhanging structures in 3D MEMS actuators to provide electrical isolation [10]. The overhanging structures can be added in the 3D design and provide self-shadowing to prevent metal from being deposited underneath during sputtering. In the second approach, we used an LPKF ProtoLaser U4 to selectively remove the deposited gold from both the substrate and printed structures. The sample was aligned using the established fiducials, and gold was removed using a laser power of 0.6 W, resulting in electrical isolation across the substrate. Both isolation approaches were used successfully in this process (Figure 4).

After laser ablation, the sample was placed on a hotplate at 70°C to release the PET substrate from the glass slide. The sample was rinsed in a bath of DI water to remove excess Crystalbond and then isopropyl alcohol was used as a final cleaning step. An example of a 42-sensor array printed using this process is shown in Figure 1, while a SEM of one of these structures is shown in Figure 4. The entire process from sensor CAD design to testing can be accomplished in a single day.

BIO-INSPIRED STRAIN SWITCH

This novel fabrication process was created to aid in developing a novel bio-inspired strain sensor designed to sense strain across a flexible wing. The sensor's design uses chevron-shaped beams [16] to mechanically amplify displacements due to strain (Figure 4). The amplified displacements close a contact switch when a specific strain threshold is reached. Unlike a traditional analog strain sensor that can provide continuous strain measurements, this new sensor design results in a digital indication of strain passing a given threshold and was inspired by the spike timing of biological campaniform sensilla [17].

The sensors' beams can be configured to detect tensile strain (Figure 1) or compressive strain (Figure 5). During printing, the pads of the sensors are isolated from one another using overhanging structures that act as self-shadowing during metal deposition. These overhangs provide local electrical isolation on the sensors. Laser ablation was then used to globally isolate the structures from one another. Global and local electrical isolation in the resulting sensors were tested using a source measure unit (SMU) instrument (2410, Keithley) and probe station (Figure 5). A contact resistance of 37 Ω was also measured by inducing a compressive strain using probes, causing the switch to close.

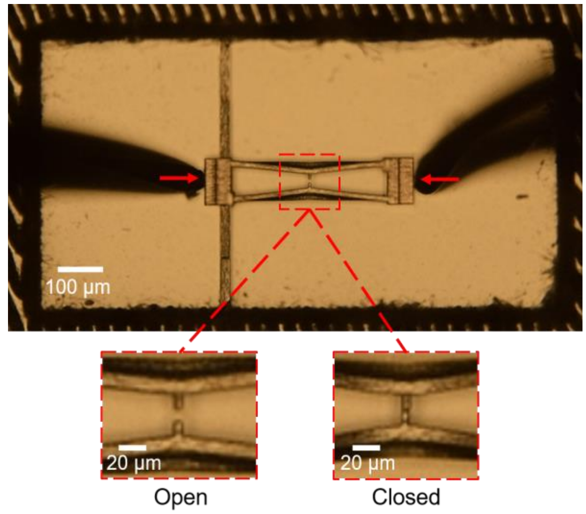

Figure 5: Activating the strain switch with probes. Arrows indicate probe direction causing strain due to compression closing the switch. Call outs zoom in on the contact area.

The sensor was tested to detect bending strain in the substrate by connecting probes directly to an Arduino Uno microcontroller. The sample was placed in a cantilever configuration with the sensors at the base of the PET cantilever (Figure 6a). A probe was used to deflect the end of the cantilever, causing a compressive strain on the top of the substrate. One side of the sensor was connected to a ground pin and the other to a digital pin on the microcontroller. An internal pull-up resistor (20 kΩ) completes the voltage divider circuit (Figure 6b). The switch is normally open when the PET is flat, registering 5V on the digital pin. The end of the PET was deflected up, resulting in a compressive bending strain that closes the switch dropping the voltage to 0V. The digital signal generated

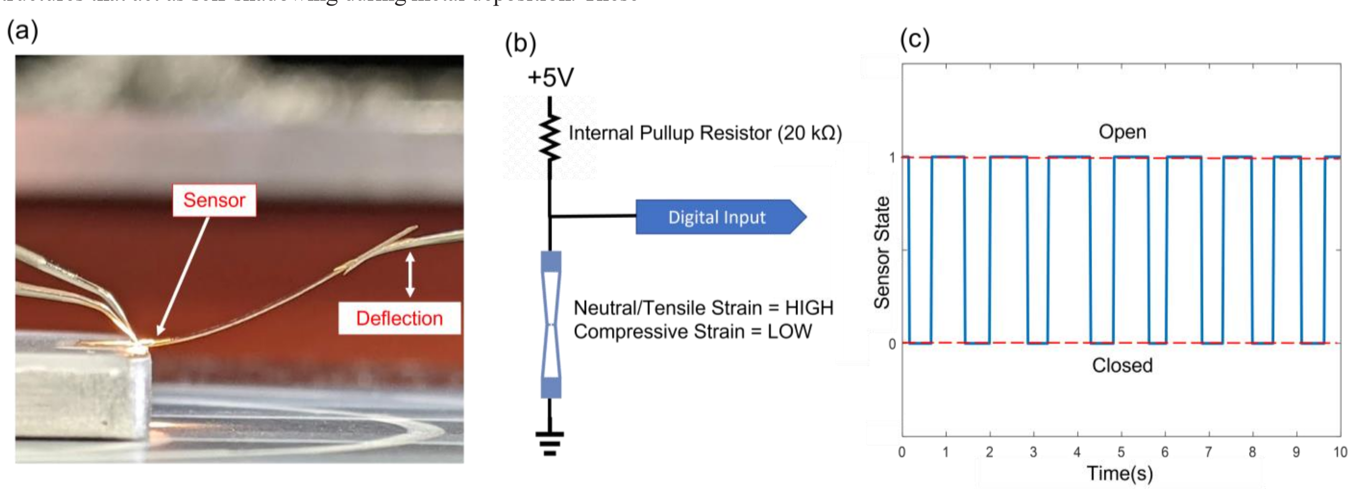

Figure 6. (a) Bending strain is tested on a probe station by deflecting the end of the PET. (b) The strain sensor replaces a switch in a voltage divider. The sensors signal can be captured by a digital pin on a microcontroller (c) Output of the digital signal from the microcontroller obtained by opening and closing the strain switch with bending strain.

from the sensor and measured on the Arduino Uno is shown in Figure 6c. Sampling the signal directly with the digital pin on the microcontroller demonstrates the ability to gain important data such as strain thresholds with precise timing and extremely low latency as compared to more traditional methods of measuring strain on wings [18]. In addition, no additional amplifiers or other circuitry is required. Similar to the biological campaniform sensilla sensors, the sensor's mechanical structure is designed to operate as a filter without requiring additional hardware.

CONCLUSION

This work presented a novel fabrication technique for 3D printing MEMS devices on highly flexible substrates. Using 3D printing, metal deposition, and laser ablation, MEMS arrays can be rapidly prototyped and tested in a single day. This fabrication process enabled the design and fabrication of a novel strain switch that activates at a specific threshold. The strain sensor uses ohmic contact as a transduction mechanism with a contact resistance of 37 Ω. The result is a sensor that requires no signal conditioning or amplification and can be observed with a digital pin on a simple microcontroller. This novel fabrication process opens the door for new and exciting MEMS devices in flexible applications.

ACKNOWLEDGEMENTS

This work is supported by NSF GRFP DGE1745016/ DGE2140739 and the Air Force Office of Scientific Research MURI award number FA9550-19-1-0386. The authors would like to thank the staff of the Claire & John Bertucci Nanotechnology Laboratory and Soft Lithography Lab at Carnegie Mellon University. Special thanks are given to Christina Kubicek for her help with photography.

REFERENCES

[1] J.-c. Tsai et al., "The evolution of mems displays," IEEE Transactions on Industrial Electronics, vol. 56, no. 4, pp. 1057–1065, 2008.

[2] M. Ahmed, I. E. Gonenli, G. S. Nadvi, R. Kilaru, D. P. Butler, and Z. Celik-Butler, "Mems sensors on flexible substrates towards a smart skin," SENSORS, 2012 IEEE, pp. 1–4, 2012.

[3] A. Tomar and Y. Tadesse, "Multi-layer robot skin with embedded sensors and muscles," in Electroactive Polymer Actuators and Devices (EAPAD) 2016, vol. 9798. SPIE, 2016, p. 979809.

[4] H.-S. Shin, Z. Ott, L. G. Beuken, B. N. Ranganathan, J. S. Humbert, and S. Bergbreiter, "Bio-inspired large-area soft sensing skins to measure uav wing deformation in flight," Advanced Functional Materials,vol. 31, no. 23, p. 2100679, 2021.

[5] E. Koch and A. Dietzel, "Skin attachable flexible sensor array for respiratory monitoring," Sensors and Actuators A: Physical, vol. 250, pp. 138–144, 2016.

[6] L. Zhang, Y. Jiang, B. Liu, M. Zhang, and W. Pang, "Highly flexible piezoelectric mems resonators encapsulated in polymer thin films," in 2018 IEEE Micro Electro Mechanical Systems (MEMS). IEEE, 2018, pp. 170–173.

[7] X. Yang and M. Zhang, "Review of flexible microelectromechanical system sensors and devices," Nanotechnology and Precision Engineering, vol. 4, no. 2, p. 025001, 2021

[8] Y. Lin, R. Zhou, and J. Xu, "Superhydrophobic surfaces based on fractal and hierarchical microstructures using two-photon polymerization: toward flexible superhydrophobic films," Advanced Materials Interfaces, vol. 5, no. 21, p. 1801126, 2018.

[9] I. Fiorello, O. Tricinci, G. A. Naselli, A. Mondini, C. Filippeschi, F. Tramacere, A. K. Mishra, and B. Mazzolai, "Climbing plant-inspired micropatterned devices for reversible attachment," AdvancedFunctional Materials, vol. 30, no. 38, p. 2003380, 2020.

[10] S. Kim, C. Velez, R. S. Pierre, G. L. Smith, and S. Bergbreiter, "A two-step fabrication method for 3d printed microactuators: characterization and actuated mechanisms," Journal of Microelectromechanical Systems, vol. 29, no. 4, pp. 544–552, 2020.

[11] B. R. Aiello, K. E. Stanchak, A. I. Weber, T. Deora, S. Sponberg, and B. W. Brunton, "Spatial distribution of campaniform sensilla mechanosensors on wings: form, function, and phylogeny," Current opinion in insect science, vol. 48, pp. 8–17, 2021.

[12] B. T. Hinson and K. A. Morgansen, "Gyroscopic sensing in the wingsof the hawkmoth manduca sexta: the role of sensor location and directional sensitivity," Bioinspiration & biomimetics, vol. 10, no. 5,p. 056013, 2015.

[13] T. L. Mohren, T. L. Daniel, S. L. Brunton, and B. W. Brunton, "Neural-inspired sensors enable sparse, efficient classification of spatiotemporal data," Proceedings of the National Academy of Sciences, vol. 115, no. 42, pp. 10 564–10 569, 2018.

[14] R. Kubicek, M. Babaei, and S. Bergbreiter, "Keeping it simple: Bio-inspired threshold-based strain sensing for micro-aerial vehicles," in 2021 IEEE/RSJ International Conference on Intelligent Robots and Systems (IROS). IEEE, pp. 7505–7511.

[15] J. S. Oakdale, J. Ye, W. L. Smith, and J. Biener, "Post-print uv curing method for improving the mechanical properties of prototypes derived from two-photon lithography," Optics express, vol. 24, no. 24, pp. 27 077–27 086, 2016.

[16] J. Guo, M. Suster, D. J. Young, and W. H. Ko, "High-gain mechanically amplified capacitive strain sensor," in SENSORS, 2005 IEEE. IEEE, 2005, pp. 4–pp.

[17] B. H. Dickerson, Z. N. Aldworth, and T. L. Daniel, "Control of moth flight posture is mediated by wing mechanosensory feedback," Journal of Experimental Biology, vol. 217, no. 13, pp. 2301–2308, 2014.

[18] Shin, Hee-Sup, et al. "Sensing skin for detecting wing deformation with embedded soft strain sensors." 2016 IEEE sensors. IEEE, 2016.

CONTACT

*R. Kubicek, rkubicek@andrew.cmu.edu